Applied Physics A (2026) 132:102
https://doi.org/10.1007/s00339-025-09234-y

Applied Physics A
Materials Science & Processing

Effect of silver addition on the structure of microwave-synthesized Cu-Ag solid solutions for organic pollutant degradation

Hanene Mehani[1] · Souad Djerad[1] · Safia Alleg[2] · Lakhdar Abadlia[3,4] · Mourad Ibrahim Daoudi[2,5] · Daniela Caschera[6]

Received: 10 September 2025 / Accepted: 10 December 2025

Abstract

This study reports the one-pot microwave synthesis of Cu-Ag powders with varying copper-to-silver molar ratios (10:1, 5:1, 2:1, and 1:1) via the reduction of copper and silver salts using ascorbic acid. The resulting products were systematically analyzed using X-ray diffraction (XRD), scanning electron microscopy (SEM), energy-dispersive X-ray spectroscopy (EDS), and electrical resistivity measurements. XRD results reveal the coexistence of Cu-rich Cu(Ag) and Ag-rich Ag(Cu) solid solutions, with the weight fraction of Cu(Ag) decreasing as Ag content increases. The crystallite size ranges from 82 to 231 nm. Increasing Ag content disrupts the Cu lattice, enhances electron scattering, and reduces charge carrier mobility, leading to a significant increase in electrical resistivity, with $\rho = 3.14\ \Omega\cdot$cm for CuAg10/1 and 6.71 $\Omega\cdot$cm for CuAg 1/1. The solid solutions display an oxidizing property in aqueous medium, which diminishes as Ag content increases. The oxidation of Methylene Blue (MB), used as a test molecule, occurs via an indirect process where the powder generates hydroxyl radicals in the acidic medium. Complete degradation of MB with CuAg 10/1 occurs within 25 min using 30 mg of the powder at 60 °C and pH 3. The processing time is further reduced to 6 min when the degradation is conducted under microwave irradiation.

Keywords Microwave-enhanced process · Ascorbic acid · Reduction method · Cu-Ag solid solutions · Heterogeneous fenton-like processes

1 Introduction

The synthesis of metals and metal oxides using microwave heating has emerged as a powerful tool in the field of materials chemistry. Microwave heating is achieved through the interaction of microwave radiation with polar molecules that possess dipole moments, causing them to rotate and create localized hot spots within the irradiated medium. Consequently, the rapid and uniform heating accelerates the progress of the chemical reactions taking place in the medium. This feature has made microwaves a highly attractive method for the synthesis of nano- and microparticles due to their ease of execution and sustainability [1].

The field of materials synthesis has been the subject of extensive research. Different metal precursors, reagents, additives, and synthesis methods have been used to prepare materials for specific applications. Copper and silver are extensively studied due to their unique chemical properties, making them suitable for various electronic, optical, medical, and catalytic applications. One of their uses includes the oxidation of contaminating organic species in water [2–4].

✉ Souad Djerad
souad.djerad@univ-annaba.dz

1 Laboratory of Environmental Engineering, Department of Process Engineering, Badji Mokhtar University, Annaba 23000, Algeria

2 Laboratory of Magnetism and Solid Spectroscopy (LM2S), Physics Department, Badji Mokhtar University, Annaba 23000, Algeria

3 Laboratory of Inorganic Materials Chemistry (LIMC), Badji Mokhtar University, Annaba 23000, Algeria

4 Department of Material Sciences, Faculty of Sciences and Technologies, Mohamed Cherif Messaadia University, Souk-Ahras 41000, Algeria

5 Department of Science of Matter, Faculty of Mathematics and Computer Science and Material Science, 8 Mai 1945 University, Guelma 24000, Algeria

6 Institute for the Study of Nanostructured Materials CNR-ISMN, Strada Provinciale 35 d, N°9, Montelibretti, Roma 00010, Italy

Published online: 20 January 2026

With their low toxicity compared to other metals, the application of copper and silver in wastewater treatment helps minimize the overall footprint of wastewater treatment and address the growing need for sustainable processes.

In the literature, many studies have been reported dealing with the synthesis of copper and silver under microwave heating.

Veiga et al. [5] employed a conventional home microwave oven to synthesize Cu_2O and Cu nanoparticles through the chemical reduction of a cupric salt using sodium citrate in alkaline glycerol media. They produced copper and copper oxide nanoparticles in various sizes, depending on the heating duration. Galletti et al. [6] synthesized copper nanoparticles using a 2-step microwave-assisted method. They mixed Cu(II) acetate and NaOH with absolute EtOH and irradiated it in a microwave. Then, they resuspended the precipitate in ascorbic acid and NaOH, achieving stable copper powder with a diameter of 7.6 nm. Njoki et al. [7] synthesized copper-silver nanoparticles (CuAg NPs) using microwave irradiation. They conducted the experiments by reacting aqueous solutions of copper nitrate, silver nitrate, and sodium acrylate at different temperatures, resulting in nanoparticles with varying sizes and shapes. Despite various synthesis methods reported in the literature, simple chemical formulations of the resulting products are commonly obtained.

In the environmental field, metals such as copper, aluminum, and iron are often involved in reactions that eliminate pollutants in aqueous environments, causing them to oxidize at the end of the processes. This fact was observed in our previous study [4], where metallic copper was partially transformed into CuO and Cu_2O after being involved in the degradation process of methylene blue.

To prevent oxidation and extend the activity of copper, it is beneficial to introduce a metal with higher chemical stability into the copper structure, thereby forming a solid solution. Solid solutions of copper-silver (CuAg) are particularly valuable in applications that require high conductivity, such as in high-field magnet windings, power transmission, and electrode materials for batteries [8–10]. However, no research has been identified that uses the solid solutions as oxidizing agents in environmental applications.

It should be noted that increasing the stability of a material does not necessarily enhance its chemical activity, as will be observed in this study. It is therefore essential to determine the optimal content of the stabilizing agent that meets both stability and activity criteria. That is the purpose of this study.

In this paper, we report on the fabrication of Cu(Ag) solid solutions using ascorbic acid under microwave heating. Ascorbic acid, known as vitamin C, is a natural water-soluble antioxidant and an essential component in biological processes used to prevent cellular damage, increase iron absorption, and promote collagen synthesis. In chemistry, ascorbic acid is regarded as a green and cost-effective reducing agent that can be utilized in various reaction systems and syntheses [11].

The resulting powders were used as generators of hydroxyl radicals for the degradation of methylene blue (MB) without needing an external oxidant. Methylene blue was chosen because it can be highly toxic when released into the environment. It can reduce light penetration and contaminate food chains for various organisms, extending to humans, causing respiratory distress, jaundice, blindness, gastrointestinal disease, and tissue necrosis [12]. This organic molecule is also highly stable and is often used to assess the efficiency of the synthesized products in the degradation processes.

In this study, the effect of increased Ag content on the physicochemical and oxidizing properties of the obtained products is described.

Additionally, we discussed the use of microwaves to speed up the degradation process of MB with the synthesized powder that contains the optimal Ag content.

2 Materials and methods

2.1 Reagents and solutions

The chemical reagents; copper sulfate $CuSO_4{\cdot}5H_2O$ (99 wt%, Sigma-Aldrich), silver nitrate $AgNO_3$ (98%, Sigma-Aldrich), and ascorbic acid $C_6H_8O_6$ (100wt%, Riedel de Haën) were employed for the powder synthesis. Methylene blue $C_{16}H_{18}ClN_3S$ (100%, Fluka) was used as a molecule test for the dye degradation. 2-propanol C_3H_8O (99.8 wt%, Fluka) and sulfuric acid H_2SO_4 (98 wt%, Biochem) were used to identify the presence of hydroxyl radicals and acidify the dye solution, respectively. Distilled water was used for the preparation of the solutions and washing.

2.2 Cu-Ag powder preparation and characterization

Four samples were synthesized by mixing 50 mL of 0.5 M copper sulfate with 50 mL of silver nitrate at the concentrations of 0.05, 0.1, 0.25, and 0.5 M, corresponding to molar ratios Cu/Ag of 10:1, 5:1, 2:1, and 1:1, respectively. The samples were labeled CuAg 10/1, CuAg 5/1, CuAg 2/1, and CuAg 1/1.

After that, 100 mL of 1 M ascorbic acid was added. Each preparation was placed into a conventional home microwave oven chamber (Electrolux, EMM1908W) and heated at 900 W for 5 min. The resulting solution was centrifuged, washed repeatedly with distilled water and ethanol, and

dried at 90 °C. XRD patterns were collected at room temperature using a PANalytical Empyrean X-ray diffractometer in a (θ-θ) Bragg Brentano configuration. Cobalt X-ray wavelengths were used for diffraction; Kα1 = 1.78901 Å, Kα2 = 1.79290 Å, and Kβ = 1.62083Å. Typical diffractometers filter out the Kβ radiation, leaving a weighted average of 1.79036 Å ((2Kα1 and Kα2)/3 = 1.79036 Å). The step size of 0.013°/min was used over the 2θ range of 10–100°. The patterns were refined using the MAUD software [13] based on the Rietveld method [14]. The morphology was examined by a scanning electron microscope (SEM, VEGAS3 TESCAN) (TESCAN, Brno, Czech Republic) combined with energy-dispersive X-ray spectroscopy (EDS) (Brucker Nano GmbH, Berlin, Germany).

2.3 Electrical resistivity measurements

The high-temperature electrical resistivity measurements of the four powders were conducted using a mass of 1 g for each sample. The powders were compacted with a mechanical press applying a load of 14 tons for 15 min. This process resulted in parallelepiped-shaped bars measuring 8 mm in thickness, 5 mm in width, and 5 mm in length. The samples were heated inside the resistivity measurement device, as described in detail in [15] to temperatures that allowed for observing various transformation stages. Both the heating and cooling rates are set at 5 °C/min to ensure complete thermal equilibrium between the measurement system and the furnace. Temperatures are measured using type K thermocouples.

The resistivity measurements were carried out by passing a direct current of 23 mA through the sample, which was connected in series with a stable reference resistor R_{stand}. The current was determined by measuring the voltage across the 0.1 Ω reference resistor. To ensure a higher quality of measurement, a current-reversing circuit was included in the setup to compensate for unwanted effects caused by thermoelectric forces. Voltages were measured using a Keithley 2001 multimeter equipped with a scanner card, providing a relative accuracy better than 0.05%. Françoise Gasser [16] developed the LabView-based control and measurement program used in this study. The resistivity of the sample ρ_{samp} is given by the following equation:

$$\rho_{samp} = \frac{U_{samp}}{U_{stand}} \frac{R_{samp}}{C} \quad (1)$$

where U_{samp} and U_{stand} are the voltages measured across the sample and the standard, C is a geometrical constant defined by the ratio $C = L/s$, where L is the length of the sample and s its cross-sectional area.

2.4 Experiments of methylene blue degradation

In a typical experiment, a definite mass of Cu-Ag powder was added to 100 mL of MB solution at a concentration of 2.10^{-5} M under heating. To maintain the uniformity of the system, the solution was kept under magnetic agitation at a moderate speed (100 rpm). The experiments were conducted in an open backer (under air). At set intervals, the solution samples were withdrawn using a syringe for absorbance measurements with the spectrophotometer, and then returned to the solution.

The concentration of the dye was determined by using a Highwave II UV/VIS spectrophotometer at 665 nm. The degradation efficiency of MB was calculated from the difference between the initial absorbance (A_0) and the absorbance at different time intervals (A_t):

$$Degradation\ efficiency\ (\%) = \left(\frac{A_0 - A_t}{A_0}\right) \times 100 \quad (2)$$

Various factors that may influence the degradation of MB were investigated, including powder loading (10, 20, 30, and 40 mg), temperature (30, 40, 50, and 60 °C), the pH of the MB solution (3, 4, 5, and 9), water matrix (presence of chlorides, sulfates, and nitrates), and the type of water (distilled, tap, and mineral). In a subsequent phase of the experiments, microwaves were utilized to evaluate their effect on activating Cu-Ag powder for the degradation of MB.

3 Results and discussion

3.1 Powders characterization

Figure 1 displays the XRD patterns of the four synthesized powders. The diffractograms show intense and narrow diffraction peaks related to the Cu (111), Cu (200), and Cu (220) Cu in addition to the (111), (200), (220), and (311) of Ag. One notes that, as the Ag content increases, the intensity of the Ag Bragg peaks increases, while that of Cu decreases. The phases, lattice parameters, weight fractions, crystallite sizes, and occupancies were obtained from the Rietveld refinement (Table 1) of the XRD patterns through the MAUD program [13]. The Rietveld refinement was performed using face-centred cubic (fcc) Cu (lattice parameter $a_0 = 3.6145$ Å) and Ag (lattice parameter $a_0 = 4.0862$ Å) phases, with space group Fm-3 m (No. 225). The reaction between Cu and Ag leads to the formation of Cu-rich Cu(Ag) and Ag-rich Ag(Cu) solid solutions. The coexistence of the Cu(Ag) and Ag(Cu) solid solutions can be due to the solubility limit of Cu and Ag in each other. Indeed, according to the

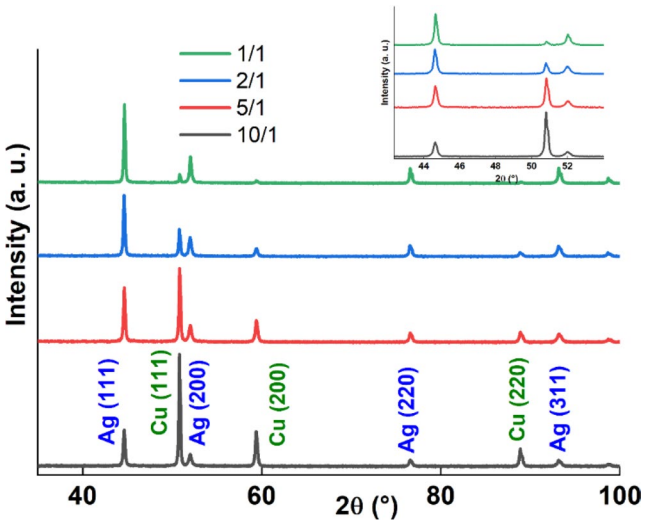

Fig. 1 XRD patterns of the Cu-Ag powders. The inset shows the enlargement in the 44–52° range

binary Cu-Ag phase diagram, the mutual solubility limit of Cu in Ag is 8.8 wt%, and that of Ag in Cu is about 8 wt% at the eutectic temperature of 779 °C [17]. This solubility limit drops to about 2 wt% Cu in Ag and 1.5 wt% Ag in Cu at a lower temperature of 500 °C. Consequently, a mixture of Cu-rich α and Ag-rich β structures can be obtained when the Ag content lies between 8 and 91.2 wt%. Furthermore, Ag and Cu atoms show atomic radii mismatch (Cu: 128 pm and Ag: 144 pm) of about 11.11%, similar fcc crystal structure, close Pauling electronegativity values (Cu: 1.90; Ag: 1.93) which supports solid solution rather than intermetallics, and similar valences (Cu: +1 and +2 commonly considered +1 in metallic bonding; Ag: +1). Therefore, Cu atoms can replace Ag atoms in the crystal lattice (and vice versa), leading to the formation of Cu(Ag) and Ag(Cu) substitutional solid solutions without significantly altering the crystal structure according to the Hume-Rothery rules.

The solubility limit of Cu in Ag, which is much higher than that of Ag in Cu, can be attributed to its smaller atomic radius compared to that of Ag. The formation of Cu(Ag) and Ag(Cu) solid solutions, rather than pure elements, is indicated by the changes in the lattice parameters and the occupancy values, as shown in Table 1. The increase in the lattice parameters of both the Cu(Ag) and Ag(Cu) solid solutions, as indicated by the relative deviation $\Delta a/a_0$, reveals that the expansion of the Cu(Ag) crystal lattice is more important than that of the Ag(Cu) solid solution. This might be related to the higher atomic radius of Ag. Furthermore, the thermal expansion can be due to the synthesis method, which induces a rapid increase in temperature due to microwave heating (900 W).

The crystallite size of the Cu(Ag) solid solution, which ranges between 105 and 144 nm, increases with decreasing Cu loading. In contrast, the crystallites composing Ag(Cu) solid solutions range between 231 and 51 nm (Table 1) and decrease with increasing Ag content.

The weight fractions show that Ag(Cu) content increased and that of Cu(Ag) decreased from the sample CuAg 10/1 to CuAg 1/1, which is consistent with the initial amounts of Cu and Ag precursors used for the preparation of the powders. Sample CuAg 10/1 primarily consists of a Cu-rich solid solution (85%) with a minor presence of an Ag-rich solid solution (15%). With the increase in Ag content (cases of CuAg 5/1 and CuAg 2/1), the proportion of Ag-rich solid solutions increased. It should be noted that the amounts of Cu used for the synthesis of the samples CuAg 5/1 and CuAg 2/1 are 5 and 2 times that of silver, respectively, which should result in the formation of higher amounts of Cu-rich solid solutions. Instead, the Cu-rich and Ag-rich solid solutions formed in almost equal parts in CuAg 5/1 and CuAg 2/1. This suggests that the reduction of Ag was more significant than that of Cu, despite the higher amount of Cu present during the synthesis. The same observation can be made for the sample

Table 1 Structural and microstructural parameters (lattice parameters, *a*, grain size, < L>, and phase proportions) obtained from the Rietveld refinement of the as-synthesized powders

Sample	Phase	a (Å) ± 10^{-4}	$\Delta a/a_0$ (%)	< L> (nm)	Occ	Weight fraction (%)
CuAg 10/1	Cu(Ag)	3.6162	0.047	105 ± 2	0.865	85 ± 0.7
	Ag(Cu)	4.0870	0.019	231 ± 4	0.244	15 ± 0.2
CuAg 5/1	Cu(Ag)	3.6165	0.055	144 ± 2	0 0.994	54 ± 0.4
	Ag(Cu)	4.0874	0.029	82.4 ± 1	0.926	46 ± 0.4
CuAg 2/1	Cu(Ag)	3.6168	0.063	131 ± 4	0.994	45.8 ± 0.6
	Ag(Cu)	4.0873	0.026	97 ± 1	0.926	54.2 ± 0.4
CuAg 1/1	Cu(Ag)	3.6166	0.058	134 ± 4	0.994	23.9 ± 0.6
	Ag(Cu)	4.0872	0.024	96 ± 1	0.926	33.3 ± 0.3
	Ag	4.0876	0.034	51 ± 1	1	42.80 ± 0.5

CuAg 1/1, for which the utilization of equimolar amounts of Cu and Ag during the synthesis resulted in the formation of a significant content of metallic Ag (42.8%), alongside Ag-rich (33.3%) and Cu-rich (23.9%) solid solutions. It seems that silver was more susceptible to being transformed into a metallic form, and the content of the Ag-rich solid solution was more important than that of the Cu-rich solid solution. Silver reduction becomes increasingly important as its concentration increases, likely because it is more easily reducible under microwave conditions than copper.

Secondary electron SEM images reveal that CuAg 10/1 consists of nearly spherical particles of approximately 1 µm in size, along with smaller particles that form fine, needle-like bunches of about 500 nm to 1 µm long (Fig. 2). As the Ag content increases, the morphology of the samples consists of spherical and hexagonal particles of varying sizes, ranging from 0.5 to 4 µm.

The EDS results obtained by mapping gave the compositions shown in Fig. 2. The weight ratios of Cu/Ag are 5.05, 2.07, 0.93, and 0.63 for CuAg 10/1, 5/1, CuAg 2/1, and CuAg 1/1, respectively. The punctual EDS analysis shows that each powder exhibits a heterogeneous composition with zones containing either Ag-enriched particles or Cu-enriched particles, likely due to the formation of solid solutions, which agrees with the XRD findings.

The synthesis method used in this study is the reduction method. Ascorbic acid, when reacting with copper sulfate or silver nitrate, reduces them to their metallic form as follows:

$$Cu^{2+} + C_6H_8O_6 \rightarrow Cu + C_6H_6O_6 + 2H^+ \quad (3)$$

$$2Ag^{+} + C_6H_8O_6 \rightarrow 2Ag + C_6H_6O_6 + 2H^+ \quad (4)$$

Water and ascorbic acid molecules are polar, and this polarity causes them to rotate rapidly when subjected to microwave radiation (MW), resulting in dielectric heating. Cu^{2+} and Ag^{+} ions do not absorb microwaves, but they can influence the ionic conductivity and overall dielectric properties of the solution.

The 900 W microwave power used for synthesis likely generates a temperature in the solutions of about 90 °C, which is not as high as that required for the high solubility of the two ions in each other. However, other parameters, such as the volume of water, the duration of microwave exposure, the molar ratio of metals, and the reducibility of metallic ions, inevitably impacted the structures of the obtained powders.

3.2 Electrical properties

Both Cu and Ag are known as electrical conductors, but their combination into a solid solution affects this property. Figure 3a shows the resistivity as a function of temperature for the four samples during the heating process. As the temperature rises from room temperature to approximately 92 °C, the electrical resistivity of all samples increases, indicating a positive temperature coefficient over 18 min. Following this, there is a rapid decrease in resistivity up to 300 °C. This behavior may be attributed to the rearrangement of the grain surface, enhanced interparticle contact that improves electrical conductivity, and powder compaction.

Above 300 °C, all samples reach very low resistivity values, reflecting the typical behavior of metals. The plateau indicates that, once the microstructure is stabilized, electrical conduction is dominated by the intrinsic metallic behavior of the CuAg solid solutions, with phonon scattering becoming the main mechanism. Moreover, the powder compaction process, which results in a density lower than that of bulk materials, also contributes to higher resistivity, particularly when interparticle diffusion is limited. The curves may thus display a positive slope at high temperatures if thermal densification occurs, such as partial grain welding under heat.

Figure 3b shows the first measurement cycle of electrical resistivity during the cooling process from 650 °C down to room temperature for the four samples. The resistivity exhibits a nearly linear decrease with decreasing temperature, which is characteristic of enhanced electron scattering due to thermal vibrations. At room temperature (Fig. 4), the electrical resistivity of Cu(Ag) solid solutions increases with the molar ratio of silver. The CuAg 10/1 displays the lowest resistivity among the tested samples ($\rho \approx 3.15$ µΩ.cm). This value differs from that of pure copper (1.68 µΩ.cm) and silver (1.59 µΩ.cm) [15, 18–20], indicating the presence of structural disorder [21].

This suggests that the addition of Ag has an impact on the electronic structure of the Cu. This is particularly true at higher Ag contents, which significantly disturb the copper lattice as silver atoms enter into solid solution, thereby enhancing electron scattering and reducing charge carrier mobility. This leads to a notable increase in electrical resistivity. Additionally, the decreasing slope of the resistivity–temperature curves observed in solid solutions with lower Ag content indicates improved thermal stability of the metallic lattice under these conditions. Therefore, despite both Cu and Ag being excellent electrical conductors, the introduction of Ag into Cu acts as a scattering center, increasing resistivity through both impurity scattering and structural disorder effects. Thus, it can be concluded that the resistivity increases with temperature for all solid solutions, which is typical of metallic behavior. At low Ag content, the conductivity is enhanced, while at high content, it induces disorder that increases resistivity. The samples CuAg 5/1 or CuAg 10/1 may represent an optimal balance between electrical conductivity and thermal stability.

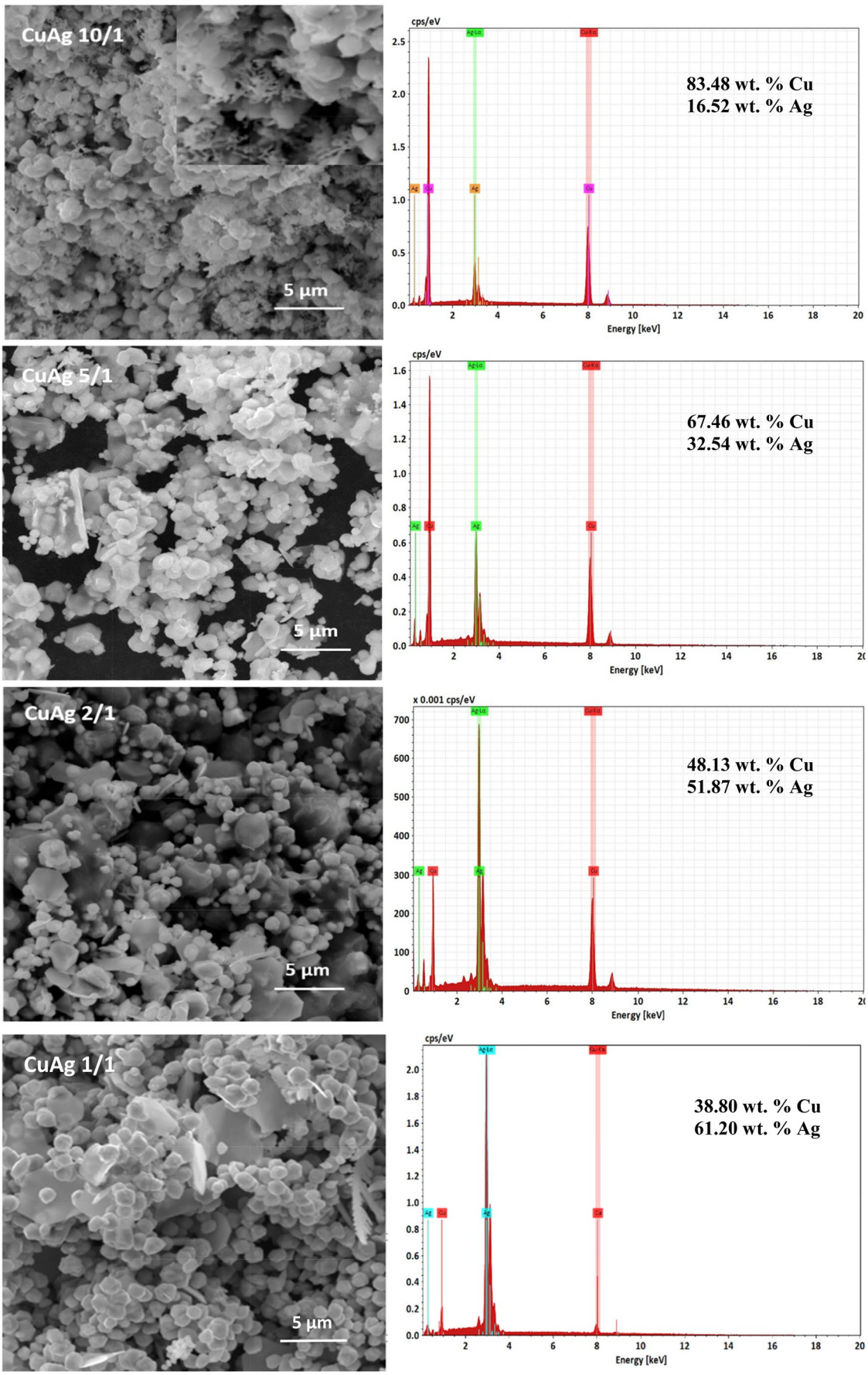
CuAg 10/1
5 µm
cps/eV
83.48 wt. % Cu
16.52 wt. % Ag
Energy [keV]
CuAg 5/1
5 µm
cps/eV
67.46 wt. % Cu
32.54 wt. % Ag
Energy [keV]
CuAg 2/1
5 µm
x 0.001 cps/eV
48.13 wt. % Cu
51.87 wt. % Ag
Energy [keV]
CuAg 1/1
5 µm
cps/eV
38.80 wt. % Cu
61.20 wt. % Ag
Energy [keV]

Fig. 2 SEM images and the corresponding EDS spectra of the CuAg powders

3.3 Application of Cu-Ag powders in methylene blue degradation

A series of initial tests was conducted to evaluate the powder's effectiveness in methylene blue (MB) degradation. The results indicated that the degradation reaction was insignificant at neutral and alkaline pH, even after an extended reaction time. However, the reaction was feasible under acidic conditions; therefore, all experiments were performed at pH 3 using H_2SO_4. The four synthesized powders were evaluated under the following conditions: 60 °C, 100 rpm, and MB concentration of 2×10^{-5} mol/L, using 30 mg of each powder. The degradation process was monitored over 60 min.

The results show that CuAg 5/1 exhibited the highest degradation efficiency, closely followed by CuAg 10/1, as both reached total degradation efficiency within 25 min (Fig. 5). The sample CuAg 2/1 showed a moderate degradation rate, gradually reaching a maximum of 90.94% after 60 min, while CuAg 1/1 displayed lower activity, registering 69.87% after the same reaction time.

The results of the solid solutions were compared to those of pure metals Cu and Ag, synthesized with the same method. It can be seen that Cu was more active than CuAg 1/1, achieving 88.92% after 60 min, while no degradation of MB was observed with Ag, even after extending the reaction time. Silver is one of the most stable metals that resists corrosion and does not easily lose electrons. The presence of 42.8% of Ag in CuAg 1/1 may be the cause of its slight efficiency in MB degradation. Therefore, incorporating silver into the solid solution structure is more beneficial than its presence in metallic form alongside the solid solution. Nevertheless, the Ag content must remain low in the solid solution to maintain high powder efficiency, as seen in CuAg 10/1 and CuAg 5/1.

In the literature, the synthesis of CuAg components has been reported using various methods. Most studies indicated that the products obtained were primarily used as catalysts rather than as oxidizing agents. For example, Tantawy et al. [22] synthesized Cu-Ag nanoparticles with three compositions ($Ag_{25}Cu_{75}$, $Ag_{50}Cu_{50}$, and $Ag_{75}Cu_{25}$) through a reduction method using hydrazinium chloride in an alkaline medium. They found that when applied in the degradation of MB as catalysts for activating H_2O_2, these had yields of 70, 65, and 43%, respectively, while monometallic components Ag and Cu showed degradation efficiencies of 31% and 10%, respectively. Padre et al. [23] synthesized Cu, Ag, and CuAg nanoparticles via a reduction method using ascorbic acid and KBH_4. They used the obtained powders as catalysts for degrading Rhodamine B, registering yields of 53.64% for Ag, 92.44% for Cu, and 97% for CuAg. Another study by Wu et al. [24] reported the synthesis of CuAg bimetallic nanoparticles with varying Cu: Ag molar ratios, using a reduction method with hexadecylamine and glucose. They found that bimetallic NPs exhibited higher activity than the monometallic Cu and Ag NPs. These results align with our findings but lack detailed information about the structure of the products. In fact, the combination of Cu and Ag in these studies was simply represented as CuAg without investigating the possibility of the formation of solid solutions.

Although the relationship between electrical conductivity and oxidation properties is not reported in the literature, it is worth noting that the samples with the lowest electrical resistance (highest electrical conductivity), CuAg 5/1 and CuAg 10/1, are those that produced the best MB degradation results.

The results for CuAg 5/1 and CuAg 10/1 are quite similar, although their synthesis costs differ. CuAg 5/1 was synthesized by using a mixture of salts composed of 83.33% copper and 16.67% silver, while the synthesis of CuAg 10/1 required 90.9% copper and only 0.091% silver. Given their comparable effectiveness and for economic considerations, CuAg 10/1 was chosen to investigate the effect of the parameters that may affect the degradation process of Methylene blue (MB).

The first parameter studied is the effect of powder loading. Figure 6a shows the results of MB degradation under the conditions: 60 °C, 100 rpm, and MB concentration of 2×10^{-5} mol/L while varying the amount of CuAg 10/1 (10, 20, 30, and 40 mg). The results show that increasing the powder loading led to improved degradation of MB. The total degradation was achieved with 40 and 30 mg after 25 min, while 90.52% and 73.19% were attained with 20 and 10 mg, respectively, after the same reaction time.

The degradation of methylene blue in the presence of the powder followed the pseudo-first-order reaction rate, for which the following equation may be used:

$$1n(\frac{A}{A_0}) = -k.t \tag{5}$$

where ″k″ is the rate constant (min^{-1}) and ″t″ is the reaction time (min), A and A_0 are the absorbance at t_0 and t.

The rate constant increased from 0.081 min^{-1} with 10 mg to 0.141, 0.219, and 0.192 min^{-1} with 20, 30, and 40 mg, respectively. The loading of 30 mg was chosen for the remaining experiments because it yielded the highest degradation efficiency.

The effect of temperature was investigated in the range of 30–60 °C using 30 mg of the powder and 100 rpm. The results show that the degradation was rapidly improved when the temperature increased from 30 to 60 °C. At 30 °C,

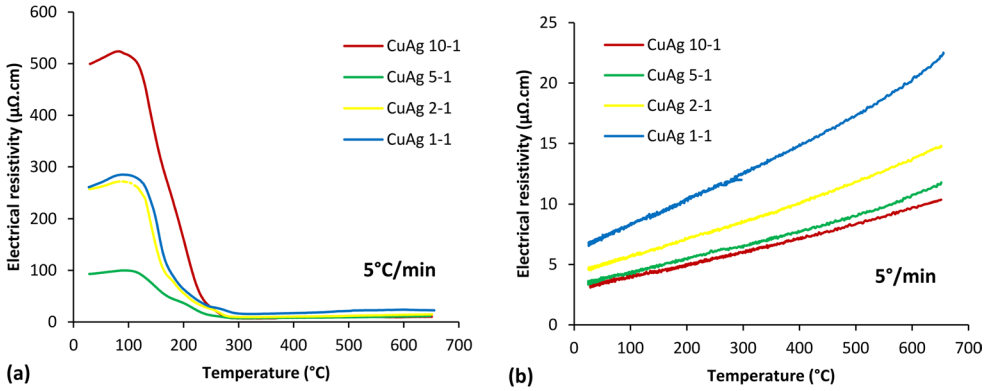

Fig. 3 Electrical resistivity variation of the CuAg powders as a function of temperature during heating (27 °C to 650 °C) (a) and cooling (650 to 27 °C) (b) cycles

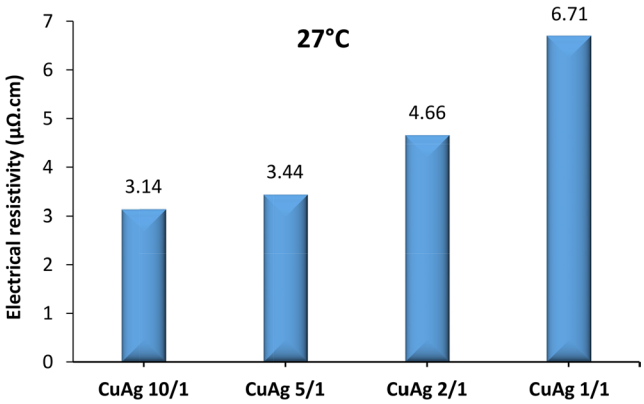

Fig. 4 Electrical resistivity of CuAg powders measured at room temperature

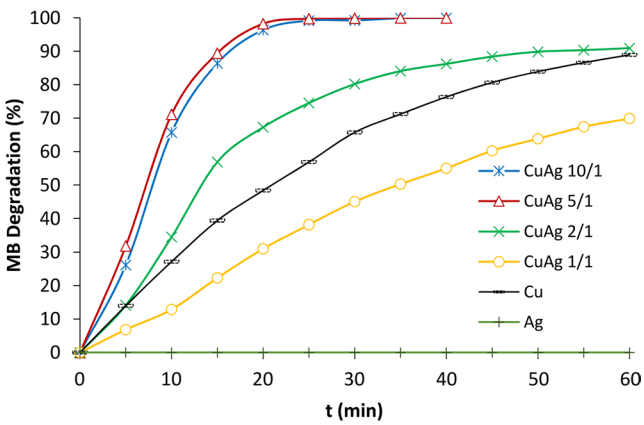

Fig. 5 Degradation of MB in the presence of the synthesized powders

the reaction was slow, reaching 92.54% after 120 min, while total degradation was achieved after 50 min at 40 °C and after 30 and 25 min at 50 °C and 60 °C, respectively (Fig. 6b).

Equation 6 was applied to the results of the effect of temperature (in Fig. 6b) to determine the activation energy by the Arrhenius equation:

$$k = A.e^{\frac{-Ea}{R.T}} \quad (6)$$

The Arrhenius equation was plotted as ln k versus (1/T) for each temperature, and the activation energy was calculated from the slope, -Ea/R. The activation energy was found to be 58.52 kJ/mol. This high value suggests that MB degradation is chemically controlled and that the powder required thermal activation to be effective. Since the activity of the synthesized powder was temperature-sensitive, a temperature of 60 °C was maintained for the remaining experiments.

The effect of the pH was studied in the pH range 3–9 using 30 mg of the powder at 60 °C and a magnetic stirring of 100 rpm. The results show that MB degradation was strongly dependent on the solution pH (Fig. 6c). It increased rapidly with increasing the acidity of the dye solution, reaching 1.71, 9.93, 69.46, and 100% after 25 min at pH 9, 5, 4, and 3, respectively, corresponding to rate constants of 0.0012, 0.0044, 0.0874, and 0.219 min^{-1}. The reaction rate at pH 3 was 182.5, 49.77, and 2.5 times faster than those registered at pH 9, 5, and 4, respectively.

This study is a continuation of our previous work [4] in which we synthesized copper using sodium ascorbate, an eco-friendly reducing agent. We found that copper produced in situ, hydroxyl radicals in the acidic medium, which are responsible for the oxidation of the organic contaminants in water.

This method is a heterogeneous Fenton-like process, which belongs to the advanced oxidation processes (AOPs) characterized by the in-situ generation of reactive oxygen species (ROS) that oxidize target pollutants [25]. Hydroxyl radicals (•OH) are one of the most studied ROS in AOPs because of their strong oxidation potential (2.4 V). They can be generated in homogeneous systems by activating oxidants such as H_2O_2 (hydrogen peroxide) and S_2O_8 (persulfate) using techniques like ultrasound, ultraviolet light, or microwaves [26, 27].

Additionally, they can be produced in situ, in heterogeneous systems, by reducing oxygen in water using metals such as iron, aluminum, and copper under certain conditions [28]. The latter method is the approach used for their generation in this study.

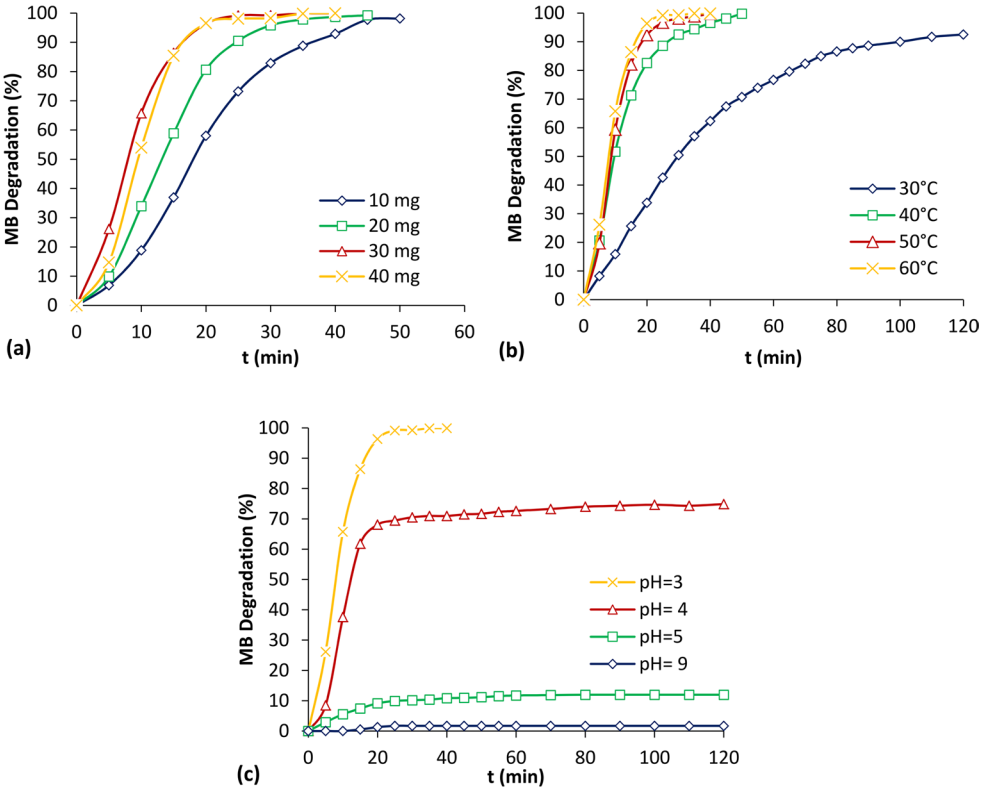

Fig. 6 Effect of powder loading (**a**), temperature (**b**), and pH (**c**) on methylene blue degradation

To assess the presence of hydroxyl radicals, 1 ml of 2-propanol, which acts as a hydroxyl radical scavenger (with a rate constant $k_{OH,\ 2\text{–propanol}} = 3 \times 10^9\ M^{-1}\ s^{-1}$) [29], was added to the methylene blue (MB) solution before starting the reaction with CuAg 10/1. The experiment was conducted at 60 °C, using 30 mg of the powder and MB solution at pH 3. No decrease in the absorbance values of MB was observed, indicating that hydroxyl radicals have been cached by the alcohol and consequently the degradation had not occurred. This result supports the conclusion that the degradation of MB is a hydroxyl radical-based oxidation system.

In this system, copper present in CuAg 10/1 with its redox potential (+0.34 V, Cu^{2+}/Cu), produced hydroxyl radicals (•OH) via the reduction of oxygen in water to form H_2O_2 (0.7 V, O_2/H_2O_2):

$$Cu \rightarrow Cu^{+} + e^{-} \tag{7}$$

$$Cu \rightarrow Cu^{2+} + 2e^{-} \tag{8}$$

$$O_2 + 2H^{+} + 2e^{-} \rightarrow H_2O_2 \tag{9}$$

$$Cu^{+} + H_2O_2 \rightarrow Cu^{2+} + OH^{-} + {}^{\bullet}OH \tag{10}$$

However, a clear mechanism for the production of radicals from silver particles is still somewhat uncertain. Some studies showed that silver required the presence of hydrogen peroxide (externally added) to generate hydroxyl radicals [30, 31] in acidic medium, while other studies reported that the in-situ production of •OH from Ag powder occurred when Ag comes into contact with oxygen, generating H_2O_2 via the production of superoxide $O_2^{-\bullet}$ [32, 33]:

$$Ag + O_2 \rightarrow Ag^{+} + O_2^{-\bullet} \tag{11}$$

$$O_2^{-\bullet} + 2H^{+} \rightarrow H_2O_2 \tag{12}$$

Hydroxyl radicals can then be formed via the reaction of silver particles and oxygen peroxide [34]:

$$Ag + H_2O_2 \rightarrow Ag^{+} + OH^{-} + {}^{\bullet}OH \tag{13}$$

It is important to note that in the CuAg 10/1 sample, copper and silver exist as solid solutions, which complicates predictions about their reactivity. However, since radicals are formed, this suggests that the mechanisms behind their production remain the same, with some effects resulting from the incorporation of copper and silver into each other.

On the other hand, the point of zero charge (pH_{PZC}) of CuAg 10/1 was determined using a method reported elsewhere [35] and was found to be 6.1. In this study, all experiments were conducted at a pH of 3, which is lower than the pH_{PZC} of the synthesized powder. At pH 3, the solid surface is positively charged due to protonation, which generates an electrostatic repulsion that hinders the adsorption of the cationic MB molecules onto the surface.

Thus, the interruption of the reaction in the presence of propanol and the positive charge of the solid surface confirm that methylene blue was degraded via the formation of hydroxyl radicals generated by the powder in the acidic medium.

To assess the effect of the process conditions on the structure of the powder, the CuAg 10/1 sample was collected after the reaction, washed, dried, and analyzed by XRD (Fig. 7a).

The results show that the diffraction peaks broaden and their intensity decreases after the reaction (AR) (Fig. 7b). This is due to the involvement of the powder constituents in the degradation process, resulting in a decrease in the crystallite size for both copper and silver solid solutions, as shown in Table 2. This decrease may be attributed to the dissolution of microcrystallites and their transformation into nanosized crystallites in the acidic medium [36, 37]. The weight fractions slightly changed, and the occupancy of both solid solutions increased from 0.865 to 1 for the Cu-rich solid solution, and from 0.244 to 0.926 for the Ag-rich solid solution. This indicates a probable release of minor components from the solid solutions they initially formed.

The operating conditions may have caused changes due to surface restructuring, grain boundary interactions, lattice alterations, and external stress.

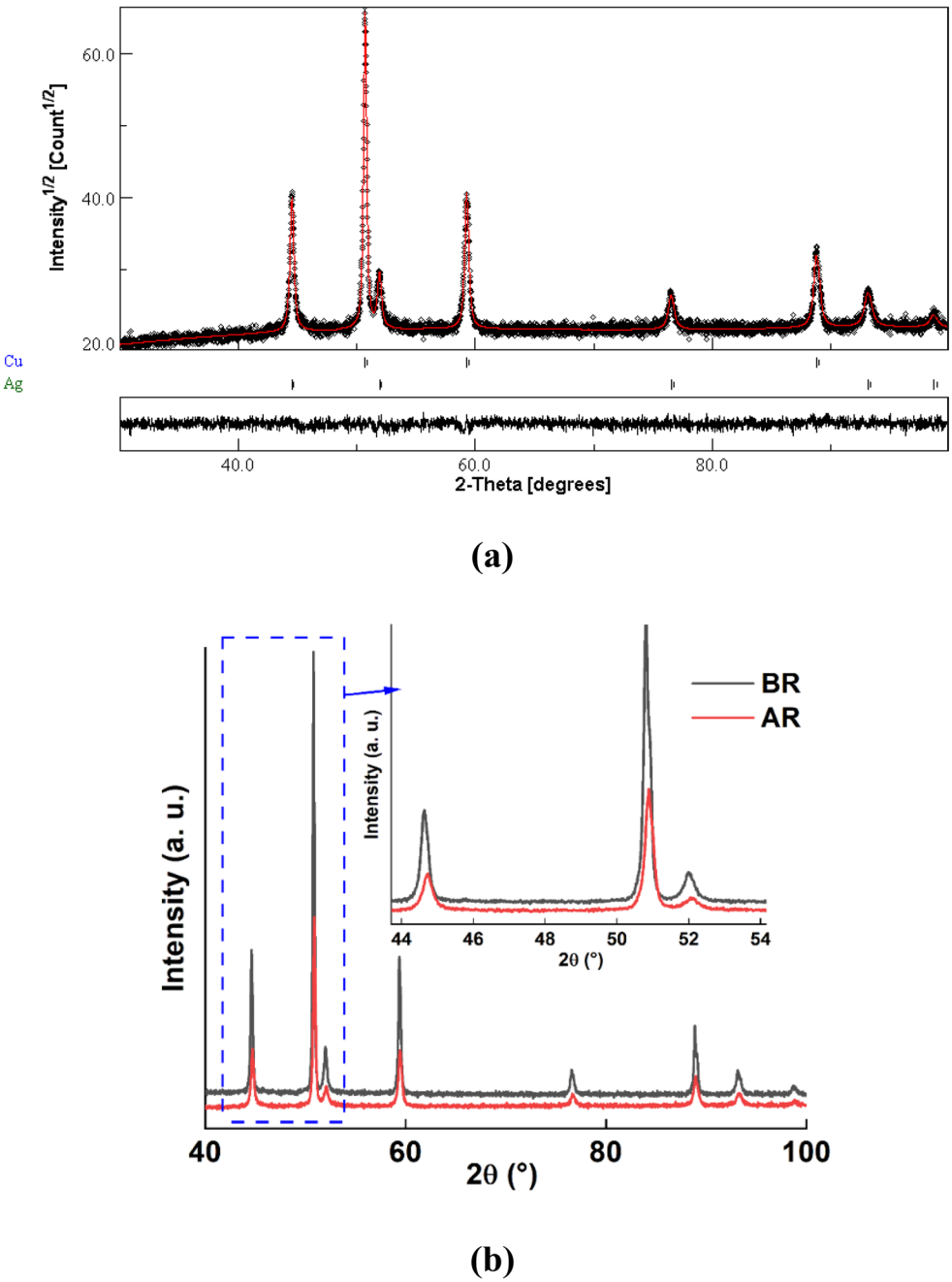

Fig. 7 *XRD* refinement pattern of the CuAg 10/1 powder after the degradation of MB (**a**) and comparison between peaks obtained before and after the degradation reaction of MB (**b**)

Table 2 Structural and microstructural parameters obtained from the XRD *Rietveld* refinement of the CuAg 10/1 powder after reaction

Sample	Phase	a (Å) ± 10^{-4}	$\Delta a/a_0$ (%)	< L>, nm	Occ.	Weight fraction (%)
CuAg 10/1 After reaction	Cu	3.6171	0.072	85 ± 1	1	89 ± 0.7
	Ag_{Cu}	4.0864	0.004	48 ± 0.6	0.926	11 ± 0.1

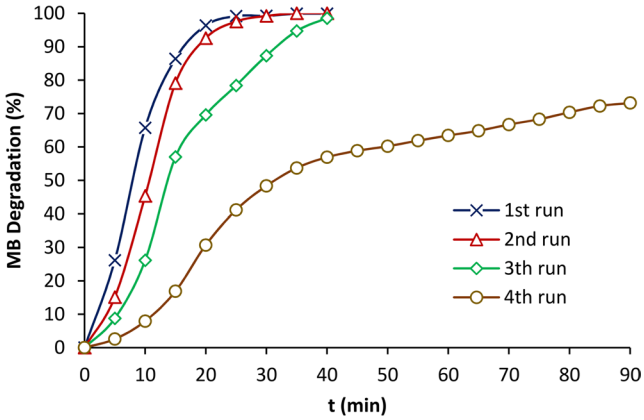

Fig. 8 MB degradation after 4 runs in the presence of CuAg 10/1

Often, a slight oxidation of Cu to Cu_2O and CuO occurs after metallic copper participates in the degradation process, as seen in our previous work [4]. However, in this study, XRD did not detect the formation of oxides. It is well known that silver offers increased resistance to oxidation and surface degradation, particularly in humid environments or at high temperatures. This high stability may have protected copper from oxidation in the harsh acidic environment, which is considered as a positive effect.

3.4 Reusability of Cu-Ag powder

To determine the stability and reusability of CuAg 10/1 powder, its performance in the degradation of MB was tested over four consecutive cycles under the same conditions (pH 3, 60 °C, 100 rpm). During the first run, the solid exhibited high efficiency by completely degrading MB within 25 min (Fig. 8).

In the second run, although the solid remained highly active, a slight decrease in the reaction rate was observed, achieving complete MB degradation within 30 min. The third run exhibited significant activity for up to 15 min, reaching 57%, after which it declined slightly and achieved total MB degradation within 40 min.

The overall activity of the powder remains high for up to 3 cycles, during which a slight decrease of about 4% was observed. A decline in activity became noticeable in the fourth run, marked by a visible slowdown in the reaction rate, which gradually decreased, reaching 73.15% after 90 min. This decline may indicate minor deactivation mechanisms, possibly due to changes in the solid surface structure as previously observed.

3.5 Effect of water matrix on the degradation of MB

Testing the synthesized sample in a mineral-rich aqueous environment that contains different dissolved compounds, is interesting, especially in a radical-driven system. Certain ions may either accelerate or slow down the radical's activity, thereby affecting the process's overall efficiency [38].

For this task, two series of experiments were conducted. In the first series, 2.10^{-3} M of NaCl, Na_2SO_4, and $NaNO_3$ were dissolved in the MB solution before the start of the experiment with CuAg 10/1. The MB solution was prepared in distilled water. The results, depicted in Fig. 9a, show that chlorides and sulfates enhanced the degradation of methylene blue, with chlorides having a more significant impact than sulfates on the degradation process, while nitrates inhibited the reaction.

In the literature, the presence of chlorides has been found to enhance the degradation process by potentially reacting with $^{\bullet}OH$ generated in this case by the matrix components to form $Cl^{\bullet}$ and $Cl_2^{\bullet-}$ [39]:

$$C1^- + {}^{\bullet}OH + H^+ \rightarrow C1^{\bullet} + H_2O \quad (14)$$

$$C1^{\bullet} + C1^- \rightarrow C1_2^{\bullet-} \quad (15)$$

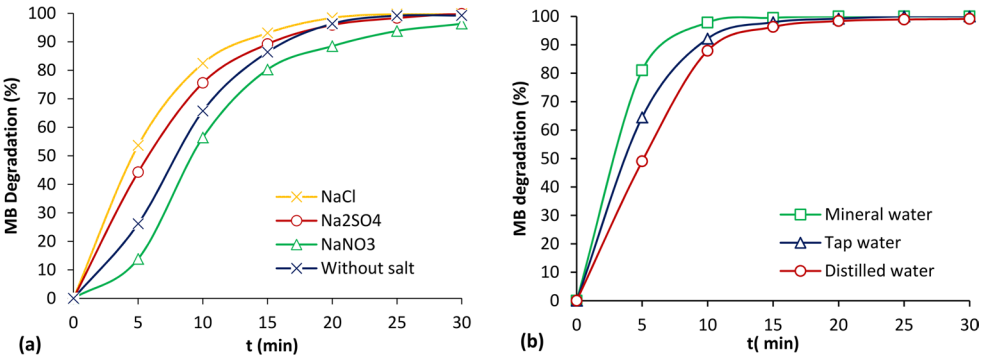

Fig. 9 Effect of inorganic ions (**a**) and the type of water (**b**) on the degradation of MB in the presence of CuAg 10/1

Chlorine radical ($Cl^{\bullet}$) possesses a high oxidation potential of 2.4 V, making it highly effective in degrading pollutants. In contrast, the chlorine radical ion ($Cl_2^{\bullet-}$) is less reactive and has a longer half-life when compared to $Cl^{\bullet}$ and $^{\bullet}OH$ [39].

The presence of the three radicals has probably improved the oxidation process in the presence of chloride anions.

Similarly, the addition of sulfates enhanced the degradation process of MB. This can be due to the formation of sulfate radicals $SO_4^{\bullet-}$ via the reaction of sulfate anions with hydroxyl radicals [38]:

$$SO_4^{2-} + {}^{\bullet}OH \rightarrow SO_4^{\bullet-} + OH^- \quad (16)$$

Sulfate radicals have a similar oxidation potential (2.5~3.1 V) to hydroxyl radicals [38]. Nevertheless, the presence of chloride ions gives better results in the oxidation of MB than sulfate ions.

The chemistry of nitrates is more complex, and their effect in the advanced oxidation processes, especially in heterogeneous systems, is poorly understood. There are some papers reporting improvement in the degradation processes in their presence [39] while others reported the contrary [40].

The results obtained in this study show that the presence of nitrates decreased the efficiency of MB degradation. Nitrate ions likely acted as $^{\bullet}OH$ quenchers, reducing their amount available for the degradation of MB, and producing nitrate radicals, which are less active than hydroxyl radicals [40]:

$$NO_3^- + {}^{\bullet}OH \rightarrow NO_3^{\bullet} + OH^- \quad (17)$$

In the second series of experiments, three types of water (mineral water, tap water, and distilled water) were used as a solvent for MB under the conditions (30 mg, 60 °C, 100 ml MB at pH 3). The results depicted in Fig. 9b show that after 5 min, the effectiveness of CuAg 10/1 in MB oxidation reached 49.02% with distilled water, 64.48% with tap water, and 81.05% with mineral water. The ionic strength of mineral water, which contained a greater concentration of mineral anions and cations compared to tap and distilled waters, has positively influenced the activity of the powder in MB degradation. This is considered a positive aspect of the activity of CuAg 10/1 powder.

The influence of inorganic anions on the efficacy of the advanced oxidation processes (AOPs) is a complex phenomenon. It is strongly linked to various factors, including the types of inorganic ions present in the bulk solution, the presence of oxidants, the characteristics of the targeted organic pollutants, and the physicochemical properties of the solid surface used in heterogeneous systems [39].

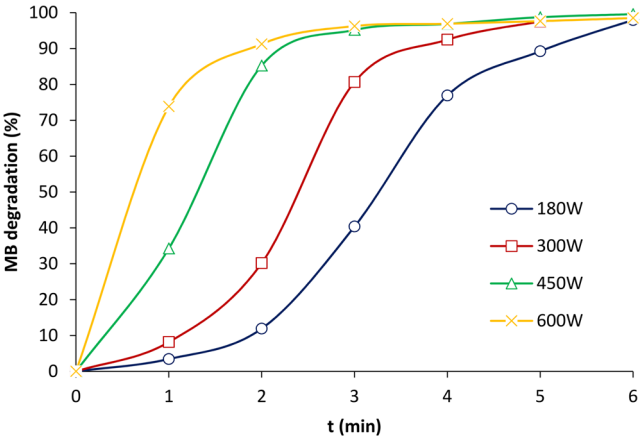

Fig. 10 Effect of microwave power on the degradation of MB in the presence of CuAg 10/1

3.6 Application of microwaves to the Cu-Ag/MB system

Processing time is a crucial parameter that can be shortened by optimizing operation conditions or adding other activating methods to accelerate the process. Microwaves are part of AOPs and have been successfully applied in various fields, including wastewater treatment, soil remediation, and sludge disposal [41, 42].

MB was completely degraded within 25 min with 30 mg of CuAg 10/1. To further shorten the reaction time, the same experiment was repeated by inserting the beaker into the same microwave oven chamber used for the synthesis of the powder. The experiment was conducted using 30 mg of the synthesized powder mixed with 100 ml of MB at pH 3, and different microwave powers were tested: 180, 300, 450, and 600 W.

The results depicted in Fig. 10 show that the degradation reaction started very quickly with 450 and 600 W registering 85.26 and 91.24% respectively after just 2 min, but it started more slowly with 300 and 180 W, and accelerated thereafter reaching rapidly total MB degradation after 6 min. The temperatures generated inside the solution by 300 and 180 W are much lower than those generated by 450 and 600 W. Despite that, a strong improvement was clearly observed with the former. This indicates that the rapid increase in reaction rate cannot be explained solely as a consequence of rapid heating. In the literature, numerous studies have postulated a so-called "microwave effect" which may outweigh the "thermal effect" of microwaves [43, 44].

To highlight the effect of the microwave irradiation, the temperatures of the solution attained after each minute were measured with the lowest power tested (180 W). The values were 33, 41.5, 48, 56, 60, and 73 °C after 1, 2, 3, 4, 5, and 6 min, respectively. At these reaction times, the MB degradation reached 3.43, 11.92, 40.38, 76.90, 89.26, and 97.96% respectively (Fig. 10).

In contrast to the MW system, where the temperature increased with time, the experiments in the water bath were kept at a constant temperature throughout the entire reaction, as shown in Fig. 6b. Taking the comparison of both systems at the same temperature of 60 °C, one can observe that with the microwaves, 60 °C was reached by the 5th minute, resulting in an 89.26% yield, while with the water bath, only 26.17% were registered at 60 °C after the same reaction time, although the experiment was carried out at 60 °C from the beginning. Despite the lower temperature to which the solution was subjected under microwaves in the range [0–5 min], the process was 3.41 times faster than that with the water bath. The cause was certainly the "microwave effect" as reported in the literature.

Although the reaction mechanism is not well understood in this case, due to the complexity of the solid solution, the utilization of microwaves has certainly facilitated the production of $^{\bullet}OH$ from the powder and, consequently, the removal of the pollutant [25].

The same experiments were repeated in a homogeneous system under the same microwave powers to verify whether microwaves alone, without the powder, could degrade MB. No decrease in absorbance values was observed.

In homogeneous systems, microwaves are applied in advanced oxidation processes to activate soluble oxidants such as H_2O_2 and S_2O_8 to generate hydroxyl radicals ($^{\bullet}OH$) or sulfate radicals ($SO_4^{\bullet-}$) [25]. In Fenton or Fenton-like processes, microwaves have been used to accelerate the production of hydroxyl radicals from the decomposition of H_2O_2 in the presence of ferrous ions (Fe^{2+}) or other metallic ions [45]. In heterogeneous systems, microwaves have been applied with various absorbing materials, including transition metal oxides, carbonaceous products, and natural mineral materials [46–48]. All these methods utilize microwaves to accelerate already active systems, but the possibility of further shortening the reaction time is explored. For example, Hu et al. [49] found that microwaves alone could not degrade p-nitrophenol (PNP), whereas their application with the persulfate (MW/PS) system removed 96.8% of PNP within 14 min.

In this study, no degradation of methylene blue was obtained using microwaves alone, suggesting that microwaves have no effect in degrading stable organic pollutants without the combination of other processes [50, 51]. The combination of CuAg 10/1 with microwaves reduced the time required for the total degradation of MB from 25 min to 6 min, thereby dividing the process duration by 4, resulting in considerable energy and time savings.

Interesting results have been achieved in this study, where solid solutions of copper and silver were used as radical generators, eliminating the need for external oxidants. The utilization of an eco-friendly and low-cost product (ascorbic acid) for the preparation, and the speed of the microwave-based synthesis method are particularly notable, as they enable the formation of solid solutions with varied compositions that can serve multiple applications in various fields.

4 Conclusion

In this study, matrices composed of several CuAg solid solutions were synthesized via a reduction process using ascorbic acid under microwave heating. The synthesis was conducted in a very short time (5 min), making this method an attractive alternative to long-term synthesis procedures.

Silver appears to be a disruptive element when introduced into copper. It causes structural disorder, raises electrical resistivity, reduces its oxidation properties at higher concentrations, but enhances thermal and chemical stability.

The powder containing the lowest silver content (CuAg 10/1) was used to generate in situ the hydroxyl radicals, which are known to break down organic pollutants. Contacting 30 mg of the powder with methylene blue at pH 3 caused the total degradation of the pollutant within 25 min, and the activity is maintained despite the ionic strength of the aqueous medium. The application of microwaves for the degradation process further reduced the time to 6 min.

The use of metals alone in the degradation processes of pollutants causes them to oxidize due to the aggressive environments used. This disadvantage can be avoided by using combinations of metals in the form of solid solutions. This approach can be implemented in the environmental field in order to combine chemical stability and efficient activity. Our results introduce CuAg solid solution with low Ag content as a promising material for organic pollutants oxidation via the heterogeneous Fenton-like process.

Acknowledgements The authors would like to thank the General Directorate of Scientific Research and Technological Development of Algeria (GDSRTD) for financial assistance.

Author contributions Hanene Mehani: Investigation, Data curation. Souad Djerad: Conceptualization, Supervision, Methodology, Writing – original draft, review & editing. Safia Alleg: Formal analysis, Data curation, Lakhdar Abadlia: Formal analysis, Data curation, Mourad Ibrahim Daoudi: Formal analysis, Daniela Caschera: Data curation.

Data availability Data will be made available on request.

Declarations

Conflict of interest The authors declare that they have no known competing financial interests or personal relationships that could have appeared to influence the work reported in this paper.

References

1. S.S. Patel, R.K. Sharma, Facile fabrication of Pluronic-mediated copper nanoparticles using microwave techniques and their application as the photocatalysts for various organic dyes degradation. Mater. Today Commun. **37**, 106990 (2023)
2. G. Palani, H. Trilaksana, R.M. Sujatha, K. Kannan, S. Rajendran, K. Korniejenko, M. Nykiel, M. Uthayakumar, Silver nanoparticles for waste water management. Molecules. **28**(8), 3520 (2023)
3. M. Sivasankari, A.J. Antonisamy, S. Malayandi, K. Rajendran, P.C. Tsai, A. Pugazhendhi, V.K. Ponnusamy, Silver nanoparticles in dye effluent treatment: a review on synthesis, treatment methods, mechanisms, photocatalytic degradation, toxic effects and mitigation of toxicity. J. Photochem. Photobiol. B **205**, 111823 (2020)
4. M. Hamidani, S. Djerad, L. Tifouti, M. Boulkra, Highly active copper in dye discoloration via a heterogeneous fenton-like process. J. Iran. Chem. Soc. **17**, 1201–1209 (2020)
5. L. Veiga, O. Garate, P. Lloret, C. Moina, G. Ybarra, One-pot ultrafast microwave-assisted synthesis of copper and copper oxide nanoparticles. Int. J. Nanosci. **18**(6), 1850034 (2019)
6. A.M.R. Galletti, C. Antonetti, M. Marracci, F. Piccinelli, B. Tellini, Novel microwave-synthesis of Cu nanoparticles in the absence of any stabilizing agent and their antibacterial and antistatic applications. Appl. Surf. Sci. **280**, 610–618 (2013)
7. P.N. Njoki, A.E. Rhoades, J.I. Barnes, Microwave-assisted synthesis of anisotropic copper–silver nanoparticles. Mater. Chem. Phys. **241**, 122348 (2020)
8. S. Piccinin, C. Stampfl, M. Scheffler, First-principles investigation of Ag-Cu alloy surfaces in an oxidizing environment. Phys. Rev. B **77**(7), 075426 (2008)
9. K. Schweinar, S. Beeg, C. Hartwig, C.R. Rajamathi, O. Kasian, S. Piccinin, M.J. Prieto et al., Formation of a 2D meta-stable oxide by differential oxidation of AgCu alloys. ACS Appl. Mater. Interfaces. **12**(20), 23595–23605 (2020)
10. A. Maleki, N. Amini, R. Rezaee, M. Safari, N. Marzban, Fabrication of Cu@Ag core-shell/nafion/polyalizarin: applications to simultaneous electrocatalytic oxidation and reduction of nitrite in water samples. Heliyon. **11**(1), e40979 (2025)
11. J. Du, J.J. Cullen, G.R. Buettner, Ascorbic acid: chemistry, biology and the treatment of cancer. BBA - Reviews Cancer. **1826**(2), 443–457 (2012)
12. P.O. Oladoye, T.O. Ajiboye, E.O. Omotola, O.J. Oyewola, Methylene blue dye: toxicity and potential elimination technology from wastewater. Results in Engineering **16**, 100678 (2022)
13. L. Lutterotti, MAUD version 2.992 (2021). http://maud.radiographema.com/
14. H.M. Rietveld, The rietveld method. Phys. Scr. **89**(9), 098002 (2014)
15. L. Abadlia, F. Gasser, K. Khalouk, M. Mayoufi, J.G. Gasser, New experimental methodology, setup and LabView program for accurate absolute thermoelectric power and electrical resistivity measurements between 25 and 1600 K. Rev. Sci. Instrum. **85**, 095121 (2014)
16. F. Gasser, Mesures automatisées de la résistivité et du pouvoir thermoélectrique absolu. Software Reg. No. R.001.190009.000 (2010)
17. P.R. Subramanian, J.H. Perepezko, The Ag-Cu (silver-copper) system. Journal of Phase Equilibria **14**, 62–75 (1993)
18. F.A. Otter, Thermoelectric power and electrical resistivity of dilute alloys of Mn, Pd, and Pt in Cu, Ag, and Au. Journal of Applied Physics **27**(3), 197–200 (1956)
19. C.E. Schuster, M.G. Vangel, H.A. Schafft, Improved estimation of the resistivity of pure copper and electrical determination of thin copper film dimensions. Microelectron. Reliab. **41**(2), 239–252 (2001)
20. R.A. Matula electrical resistivity of copper, gold, palladium, and silver. J. Phys. Chem. Ref. Data **8**(4), 1147–1298 (1979)
21. W. Li, H. Liu, Z. Hou, Z. Zhang, J. Dong, M. Wang, H. Guo, K. Song, Effect of trace silver on the conductivity and softening temperature of high conductivity and high heat resistance pure copper. J. Mater. Res. Technol. **33**, 4749–4762 (2024)
22. H.R. Tantawy, A.A. Nada, A. Baraka, M.A. Elsayed, Novel synthesis of bimetallic Ag-Cu nanocatalysts for rapid oxidative and reductive degradation of anionic and cationic dyes. Appl. Surf. Sci. Adv. **3**, 100056 (2021)
23. S.M. Padre, S. Kiruthika, S. Mundinamani, S.R. Rakivirana, J.R. Surabhi, K.M. Jeong, M.S. Eshwarappa, V. Murari, M. Shetty, S.C. Ballal, Gurumurthy, Mono-and bimetallic nanoparticles for catalytic degradation of hazardous organic dyes and antibacterial applications. ACS Omega. **7**(39), 35023–35034 (2022)
24. W. Wu, M. Lei, S. Yang, L. Zhou, L. Liu, X. Xiao, C. Jiang, V.A. Roy, A one-pot route to the synthesis of alloyed Cu/Ag bimetallic nanoparticles with different mass ratios for catalytic reduction of 4-nitrophenol. J. Mater. Chem. A **3**(7), 3450–3455 (2015)
25. A. Saravanan, V.C. Deivayanai, P. Senthil Kumar, G. Rangasamy, R.V. Hemavathy, T. Harshana, N. Gayathri, K. Alagumalai, A detailed review on advanced oxidation process in treatment of wastewater. Chemosphere **308**, 136524 (2022)
26. H. Xia, C. Li, G. Yang, Z. Shi, C. Jin, W. He, J. Xu, G. Li, A review of microwave-assisted advanced oxidation processes for wastewater treatment. Chemosphere. **287**, 131981 (2022)
27. G.P. Anipsitakis, D.D. Dionysiou, Radical generation by the interaction of transition metals with common oxidants. Environ. Sci. Technol. **38**(13), 3705–3712 (2004)
28. M. Hamidani, S. Djerad, L. Tifouti, Synthesis of copper with sodium ascorbate and its application in malachite green discoloration. J. Environ. Chem. Eng. **8**(5), 104457 (2020)
29. S.P. Sun, A.T. Lemley, p-Nitrophenol degradation by a heterogeneous fenton-like reaction on nano-magnetite. J. Mol. Catal. A Chem. **349**(1–2), 71–79 (2011)
30. D. He, C.J. Miller, T.D. Waite, Fenton-like zero-valent silver nanoparticle-mediated hydroxyl radical production. J. Catal. **317**, 198–205 (2014)
31. W. He, Y.T. Zhou, W.G. Wamer, M.D. Boudreau, J.J. Yin, Mechanisms of the pH dependent generation of hydroxyl radicals and oxygen induced by Ag nanoparticles. Biomaterials **33**(30), 7547–7555 (2012)
32. D. He, A.M. Jones, S. Garg, A.N. Pham, T.D. Waite, Silver nanoparticle–reactive oxygen species interactions: application of a charging–discharging model. J. Phys. Chem. C **115**(13), 5461–5468 (2011)
33. B.H.J. Bielski, D.E. Cabelli, R.L. Arudi, A.B. Ross, Reactivity of HO<Subscript>2</Subscript>/O<Superscript>−2</Superscript> radicals in aqueous solution. J. Phys. Chem. Ref. Data **14**(4), 1041–1100 (1985)
34. J.Z. Guo, H. Cui, W. Zhou, W. Wang, Ag nanoparticle-catalyzed chemiluminescent reaction between luminol and hydrogen peroxide. J. Photochem. Photobiol. A Chem. **193**(2–3), 89–96 (2008)
35. C.A. León y León, L.R. Radovic interfacial chemistry and electrochemistry of carbon surfaces. Chem. Phys. Carbon **24**, 213–310 (1994)
36. M.A. Behrens, A. Franzén, S. Carlert, U. Skantze, L. Lindfors, U. Olsson, On the Ostwald ripening of crystalline and amorphous nanoparticles. Soft Matter. **21**(12), 2349–2354 (2025)
37. M. Oliva-Ramírez, M. Macías-Montero, A. Borras, A.R. González-Elipe, Ripening and recrystallization of NaCl nanocrystals in humid conditions. RSC Adv. **6**(5), 3778–3782 (2016)
38. J. Wang, S. Wang, Effect of inorganic anions on the performance of advanced oxidation processes for degradation of organic contaminants. Chem. Eng. J. **411**, 128392 (2021)
39. H. Barndõk, D. Hermosilla, L. Cortijo, C. Negro, Á. Blanco, Assessing the effect of inorganic anions on TiO_2-photocatalysis

and Ozone oxidation treatment efficiencies. J. Adv. Oxid. Technol. **15**(1), 125–132 (2012)
40. K. Thomas, A. Volz-Thomas, D. Mihelcic, H.G.J. Smit, D. Kley, On the exchange of NO_3 radicals with aqueous solutions: solubility and sticking coefficient. J. Atmos. Chem. **29**, 17–43 (1998)
41. Y. Feng, Y. Tao, Q. Meng, J. Qu, S. Ma, S. Han, Y. Zhang, Microwave-combined advanced oxidation for organic pollutants in the environmental remediation. Chem. Eng. J. **441**, 135924 (2022)
42. W. Chen, Z. Luo, C. Wu, P. Wen, Q. Li, Oxidative removal of recalcitrant organics in shale gas flowback fluid by the microwave-activated persulfate process. Environ. Sci. Pollut Res. **26**, 684–693 (2019)
43. F. Langa, P. de la Cruz, A. de la Hoz, A. Díaz-Ortiz, Díez-Barra, microwave irradiation: more than just a method for accelerating reactions. Contemp. Org. Synth. **4**(5), 373–386 (1997)
44. A. De la Hoz, A. Diaz-Ortiz, A. Moreno, Microwaves in organic synthesis. Chem. Soc. Rev. **34**(2), 164–178 (2005)
45. J.J. Pignatello, E. Oliveros, A. MacKay, Advanced oxidation processes for organic contaminant destruction based on the fenton reaction. Crit. Rev. Environ. Sci. Technol. **36**(1), 1–84 (2006)
46. S. Li, G. Zhang, W. Zhang, H. Zheng, W. Zhu, N. Sun, Y. Zheng, P. Wang, Microwave enhanced fenton-like process for degradation of perfluorooctanoic acid using Pb-$BiFeO_3$/rGO as heterogeneous catalyst. Chem. Eng. J. **326**, 756–764 (2017)
47. Z. Liu, H. Meng, H. Zhang, J. Cao, K. Zhou, J. Lian, Highly efficient degradation of phenol wastewater by microwave induced H_2O_2-CuO_x/GAC catalytic oxidation process. Sep. Purif. Technol. **193**, 49–57 (2018)
48. W. Pan, G. Zhang, T. Zheng, P. Wang, Degradation of p-nitrophenol using CuO/Al_2O_3 as a fenton-like catalyst under microwave irradiation. RSC Adv. **5**(34), 27043–27051 (2015)
49. L. Hu, G. Zhang, Q. Wang, X. Wang, P. Wang, Effect of microwave heating on persulfate activation for rapid degradation and mineralization of p-nitrophenol. ACS Sustain. Chem. Eng. **7**(13), 11662–11671 (2019)
50. C. Qi, X. Liu, C. Lin, H. Zhang, X. Li, J. Ma, Activation of peroxymonosulfate by microwave irradiation for degradation of organic contaminants. Chem. Eng. J. **315**, 201–209 (2017)
51. F. Wang, C. Wu, Q. Li, Treatment of refractory organics in strongly alkaline dinitrodiazophenol wastewater with microwave irradiation-activated persulfate. Chemosphere. **254**, 126773 (2020)